

Research Article

¹Department of Anatomy & Cell Biology, McGill University, Montreal, QC, Canada

²Faculty of Dentistry, McGill University, Montreal, QC, Canada

Keywords

Osteoclasts, osteoclastogenesis, Ca^{2+} oscillations, fluorescence imaging

Email Correspondence

mariya.stavnichuk@mail.mcgill.ca

Mariya Stavnichuk¹, Gulzhakhan Sadvakassova², Svetlana Komarova^{1,2}

Fluorescence Imaging of Receptor Activator of Nuclear Factor Kappa-B Ligand-Mediated Calcium Oscillations in Osteoclasts

Abstract

Background: Numerous bone diseases are caused by abnormal activity of osteoclasts, cells responsible for physiological bone degradation. Understanding the mechanisms of osteoclast formation and activation is important for developing diagnostic tools and treatments for various bone diseases. Receptor activator of nuclear factor κB ligand (RANKL), a key osteoclastogenic cytokine, induces changes in intracellular Ca^{2+} concentration ($[\text{Ca}^{2+}]_i$) that can be visualized and measured with a fluorescent Ca^{2+} binding dye. The objective of the study was to characterize the changes in $[\text{Ca}^{2+}]_i$ induced by acute application of RANKL in osteoclast precursors.

Methods: We performed calcium imaging in osteoclast precursors generated from RAW 264.7 cells loaded with Fura-2 fluorescent dye using an inverted microscope, Nikon TE2000-U. Data was collected with Volocity software and analysed in Excel and MATLAB.

Results: In osteoclast precursors, RANKL induced oscillations in $[\text{Ca}^{2+}]_i$ within 2 minutes of exposure. The main frequency of oscillations was approximately 37.7 mHz. However, no significant change in the mean level of intracellular Ca^{2+} was observed. Interestingly, when ATP was applied to RANKL-treated osteoclast precursors, it induced a long-lasting increase in $[\text{Ca}^{2+}]_i$ compared to control cells.

Limitations: The limitations of our study included the small number of replicates and the short duration of fluorescence recording under each condition.

Conclusions: Short exposure of osteoclast precursors to RANKL not only induced oscillations in calcium concentration, but also modulated cellular response to the subsequent application of ATP.

Introduction

Bone is an organ that continuously undergoes remodelling activity to cater to the demands of the organism. Its dynamic equilibrium depends on the balance between bone-forming cells, osteoblasts, and bone-resorptive cells, osteoclasts. Understanding the underlying causes of bone homeostasis is important for developing treatments against various diseases that result from an imbalance in bone remodelling. A large number of bone diseases, such as metastatic cancers, osteoporosis, and rheumatoid arthritis arise from increased resorption of bone by osteoclasts. (1) Osteoclasts are cells of hematopoietic origin formed by differentiation of monocyte or macrophage precursors. (2) Osteoclastogenesis is initiated by receptor activator of nuclear factor κB 's (RANK) stimulation by its ligand, RANKL. (3) Activation of RANK leads to subsequent induction of co-stimulatory receptors such as the osteoclast-associated receptor (OSCAR), which results in activation of phospholipase C (PLC), and formation of inositol-1,4,5- triphosphate (IP3), which binds to its receptor on the endoplasmic reticulum releasing stored Ca^{2+} . (3) Resulting cytosolic Ca^{2+} concentration oscillations are important for stimulation of the calcineurin/NFATc1 that is essential for osteoclastogenesis. (3) In addition to RANKL, multiple other factors are known to affect osteoclast calcium, including extracellular ATP that can be produced by mechanically stimulated cells. (3) Extracellular ATP activates plasma membrane P2 purinergic receptors inducing a fast transient increase in $[\text{Ca}^{2+}]_i$. (5)

The objective of this study was to investigate changes in cytosolic Ca^{2+} concentration in response to RANK-RANKL interaction. Intracellular Ca^{2+} oscillation can be visualized using a fluorescence microscope. In this experiment, we used Fura-2, a ratio-metric fluorescent dye that binds free intracellular Ca^{2+} . The advantage of ratiometric dyes over single wavelength

dyes is that the obtained ratio is independent of the dye concentration. (4) The dye is loaded into cells in the form of as acetoxy-methyl-ester Fura-2 (Fura-2 AM) and it is de-esterified by cellular esterases, leaving Fura-2 trapped in the cell. (4) Fluorescence microscopes have an excitation filter that allows a specific excitation wavelength to go through. Excitation light is reflected from a dichromatic mirror, which directs light onto the specimen. Fura-2 has the property of being excited at 340 nm in its calcium-free form and at 380 nm when bound to Ca^{2+} . The excited sample emits light that passes through the mirror and emission filter of 510 nm for Fura-2. (4)

Methods

Cell Culture

We used RAW 264.7 cells (American Type Culture Collection) derived from a mouse leukemic monocyte macrophage cell line as osteoclast precursors. Cells were cultured at 37°C and 5% CO_2 in 2 mL DMEM (319-020-CL, Wisent Inc.) supplemented with 1% penicillin-streptomycin (450-201-EL, Wisent Inc.), 10% FBS (080-150, Wisent Inc.), and 50 ng/mL of recombinant GST-RANKL (produced in-house, 50 $\mu\text{g}/\text{mL}$). RANKL was added in order to induce differentiation of monocytes into osteoclast precursors. We plated cells at 5×10^3 cells/ cm^2 in 35 mm glass bottom cell culture dishes (MatTek Corp.). After two days, media was changed to DMEM containing 1.5 μM Fura-2 AM (F1221, Invitrogen). 30 minutes after media change, cells were washed with 1 mL DMEM buffered with 10 mM HEPES (15630-080, Gibco) and another 1 mL of HEPES-buffered DMEM was added to cells. After addition of Fura-2 AM, dishes were either covered with aluminium foil or manipulated in darkness to prevent bleaching.

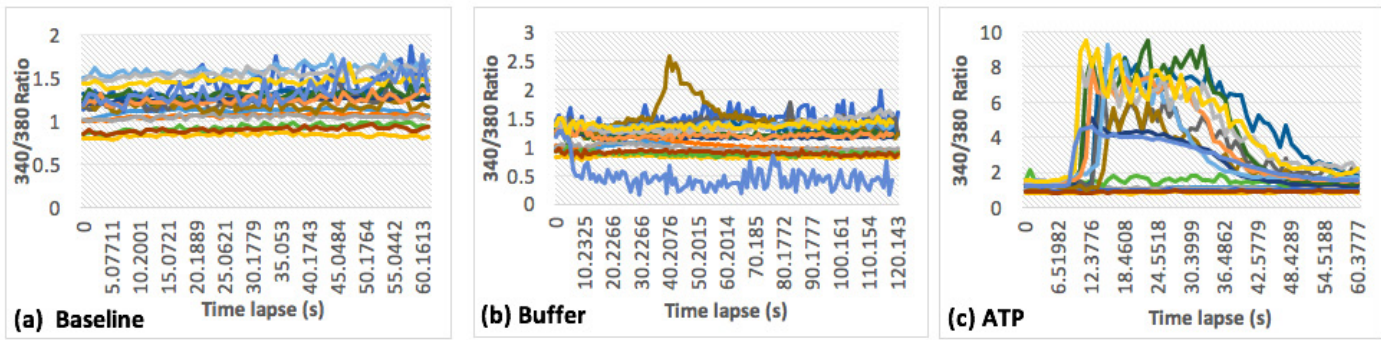


Fig. 1. Changes in $[Ca^{2+}]$ following addition of buffer. Each line graph represents single-cell fluorescence intensity ratio measurement. (A) Baseline measurements of fluorescence intensity. (B) Fluorescence intensity after addition of the buffer. (C) Fluorescence intensity after addition of ATP.

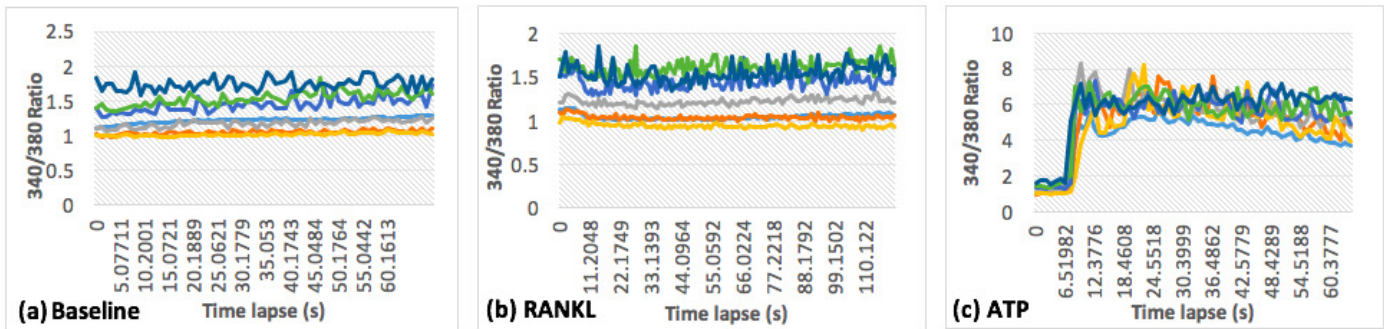


Fig. 2. Changes in $[Ca^{2+}]$ following addition of RANKL. Each line graph represents single-cell fluorescence intensity ratio measurement. (A) Baseline measurements of fluorescence intensity. (B) Fluorescence intensity after addition of RANKL. (C) Fluorescence intensity after addition of ATP.

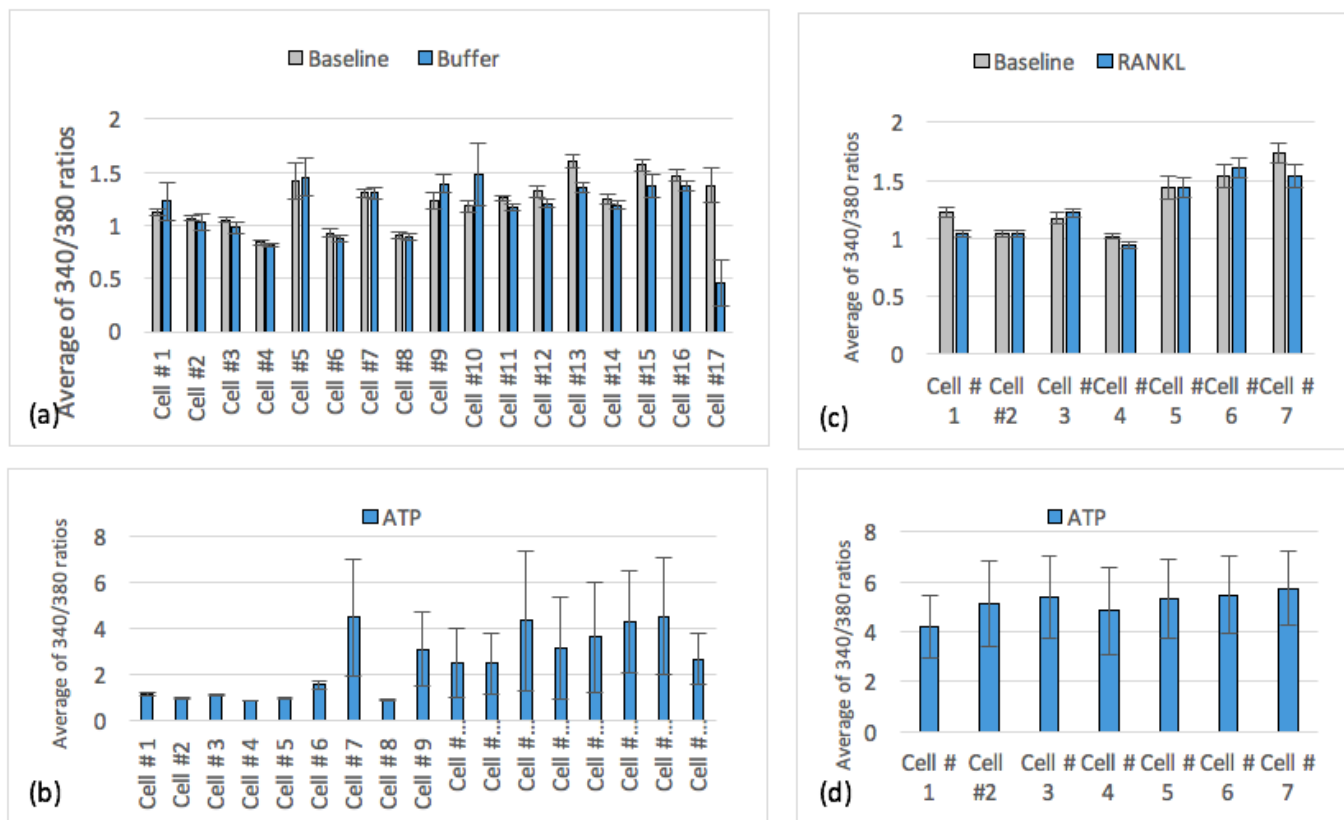


Fig. 3. Average level of $[Ca^{2+}]$ after addition of buffer, RANKL or ATP. The same cells were examined in charts (A) and (B), and in charts (C) and (D). Shown is average fluorescence intensity (A) at the baseline (grey) and after buffer addition (blue); (B) after ATP addition; (C) at the baseline (grey) and after RANKL addition (blue); (D) after ATP addition.

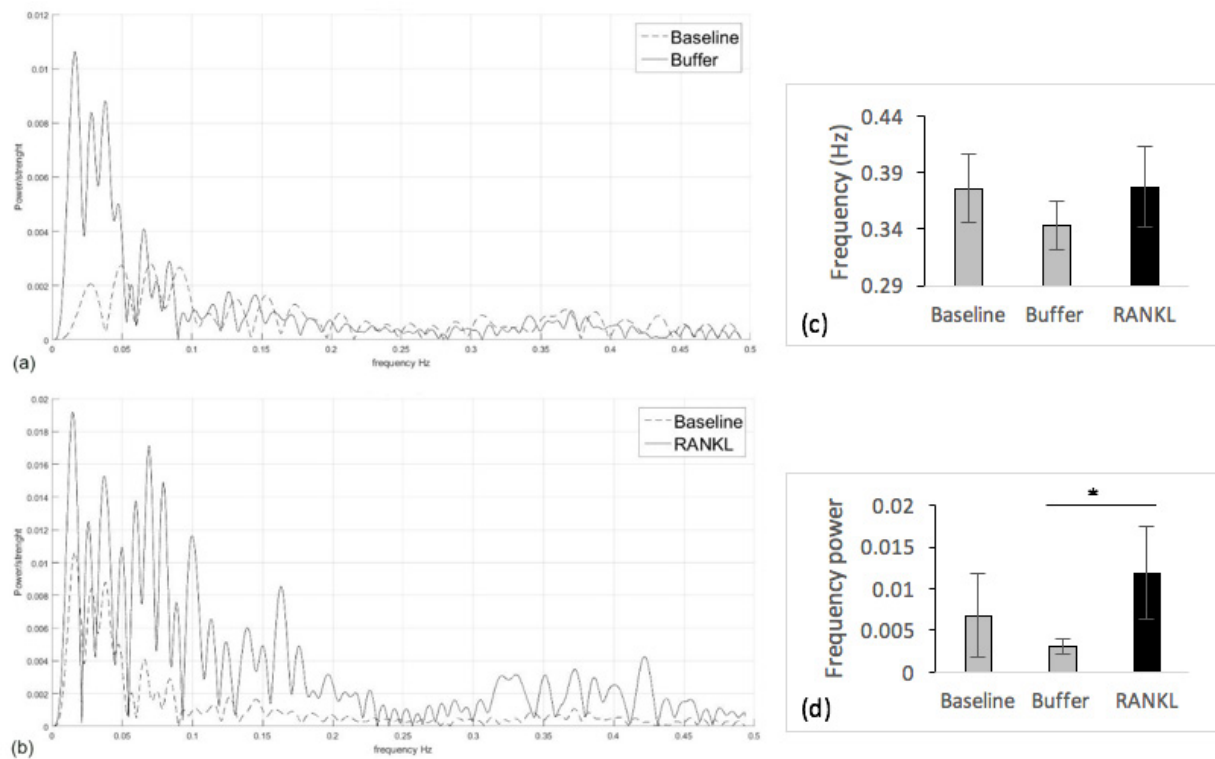


Fig. 4. Spectral analysis of $[Ca^{2+}]_i$ oscillations. Average power spectrum analysis (A) at the baseline and after buffer addition and (B) at the baseline and after RANKL addition. (C) Average dominant frequency of $[Ca^{2+}]_i$ oscillations between 20-50 mHz. (D) Average strength of dominant frequency of $[Ca^{2+}]_i$ oscillations between 20-50 mHz. Data are means \pm SD, * indicates $p < 0.05$ examined by Student's t-test.

Fluorescence Imaging

The cells were given 15 minutes to acclimatize before imaging. We performed imaging on an inverted Nikon TE2000-U microscope equipped with a cooled charge-couple device (CCD) camera (Hamamatsu) and 40X UV corrected Nikon Fluor oil immersion objective. We recorded fluorescence emission data points every second at 510 nm after excitation at 340 and 380 nm alternated by a high speed wavelength switching device (Lambda DG-4, Quorum Technologies). In each dish, the measurement consisted first of a baseline recording for one minute. Either 50 μ L of buffer solution or 50 ng/mL of RANKL was added with a micropipette six to eight seconds after the start and fluorescence intensity was recorded for two minutes. Finally, 50 μ L of 10 mM ATP was added, giving a final concentration of 10 μ M, and fluorescence was recorded for one minute. Baseline and addition of buffer were used as a negative control, whereas ATP was used as a positive control. The buffer was composed of 150 mM NaCl, 0.25 mM DTT, 0.1 mM PMSE, 25% glycerol.

Data Analysis

We performed data analysis using Excel and MATLAB R2015a software. Frequency analysis of Ca^{2+} oscillations was performed using Per Uhlén's protocol from Spectral Analysis of Calcium Oscillations. (6) Statistical significance was assessed using a two-tailed Student's t-test ($p < 0.05$).

Results

To analyse collected data, we used the region of interest (ROI) tool in Vo-lu-city software to select the cell of interest. Measurements from selected ROI were analysed and changes in $[Ca^{2+}]_i$ were expressed as a ratio of Fura-2's fluorescent intensity when excited with 340 and 380 nm wavelength (340/380 ratios). $[Ca^{2+}]_i$ oscillations were present at the baseline and after the buffer addition (Fig. 1), as well as after application of RANKL (Fig. 2). Addition of ATP caused a fast transient increase of $[Ca^{2+}]_i$ in negative control cells, that recovered by the end of recording (Fig. 1C) and a

fast long-lasting increase of $[Ca^{2+}]_i$ in RANKL stimulated cells that was observed over the entire time of recording (Fig. 2C). We computed average levels of $[Ca^{2+}]_i$ for each cell at baseline and after addition of buffer or RANKL (Fig. 3A and C). No significant difference in the average $[Ca^{2+}]_i$ was observed.

Since the frequency of oscillations appeared to change after addition of RANKL, we next performed frequency analysis using MATLAB R2015a software. Following Per Uhlén's protocol, (6) outliers were discarded. Cells that did not respond to ATP, and cells exhibiting aberrant responses to buffer or RANKL (such as single cells with a transient increase in $[Ca^{2+}]_i$ on Fig. 1B) were excluded from further analysis. To obtain spectral analy-

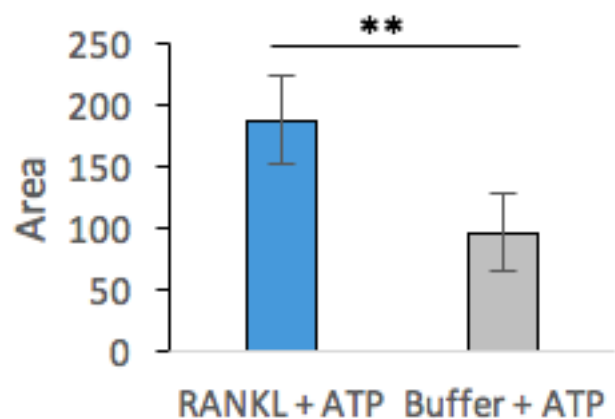


Fig. 5. Acute treatment with RANKL induced a change in a subsequent calcium responses to ATP. ATP responses following application of buffer (grey, same cells as presented on Fig. 1C) or RANKL (blue, same cells as presented on Fig. 2C) were analysed for the area under the calcium response curve. Data are means \pm SD, ** indicates $p < 0.01$ examined by Student's t-test.

sis of $[Ca^{2+}]_i$ oscillations, we applied a Hanning window function to previously acquired data to remove noise oscillation, and data was centered and analyzed using a fast Fourier Transform function. Results were displayed as a function of frequency to its relative strength (power) (Fig. 4A,B). Only the frequency of the dominant peak in the region of 20-50 mHz was chosen for analysis per single-cell measurement, as frequencies lower than 17 mHz (1/60 seconds of recording) are artifacts of the application of the Fourier Transform. Dominant peaks in the region between 20-50 mHz were 37.6 mHz for the baseline, 34.4 mHz for the buffer, and 37.7 mHz for RANKL (Fig. 4C). To compare frequencies, the average of their relative strength was analyzed. No significant difference was found between the strength of baseline and RANKL measurements. However, the Student's t-test showed significant difference in frequency strength between buffer and RANKL measurements ($p < 0.05$) (Fig. 4D).

We have noticed that the response to ATP appears to differ in cells exposed to buffer and cells exposed to RANKL. We analysed the area under the curve of the fluorescence intensity ratio using MATLAB (Fig. 5). ATP-induced calcium responses had significantly larger area ($p < 0.01$) in RANKL-stimulated cells than ATP-induced responses in the control group cells.

Discussion

The objective of this study was to examine the changes in intracellular Ca^{2+} concentration upon stimulation of osteoclast precursors by RANKL. Using live cell fluorescence imaging we determined that acute application of RANKL did not affect the frequency of calcium oscillations in osteoclast precursors, but resulted in a more prominent appearance of oscillatory behaviour. Interestingly, we also found that short treatment with RANKL significantly affected the cell response to ATP, resulting in longer-lasting release of calcium compared to control cells.

Frequency analysis showed that both the control and experimental groups had calcium oscillations at similar frequencies and with similar values of major frequency peaks. In addition, average levels of calcium were not significantly different between the experimental groups. Although these data appear to contradict the known effect of RANKL in stimulating osteoclast calcium oscillations, it is important to take into account the experimental design of our studies. It has been previously shown that RANKL induces long-lasting Ca^{2+} oscillations that can last from 24 to 48 hours after RANKL stimulation in a primary cell culture. (7) In our study, we focused on late osteoclast precursors, which were formed from RAW 264.7 cells exposed to RANKL for 48 hours prior to imaging that were then cultured without RANKL for one hour prior to acute addition of RANKL. Nevertheless, we found that acute addition of RANKL allowed the cells to maintain more prominent oscillation compared to those observed after addition of buffer, suggesting that removal of RANKL may lead to a gradual decrease in calcium oscillations in osteoclast precursors. It is also possible that a relatively short recording time did not allow us to explore the whole range of changes induced in osteoclast precursors by acute exposure to RANKL.

We observed a significant difference in calcium response to ATP between the control and RANKL stimulated cells. In both control and RANKL-treated groups, ATP induced fast elevation of calcium that reached similar maximal levels. However, unlike the control group, in the cells that were stimulated by RANKL, $[Ca^{2+}]_i$ never returned to basal level and continued to oscillate at a new higher level over the course of recording. This resulted in a significantly higher area under the curve of Ca^{2+} concentration response, indicative of a higher cumulative amount of Ca^{2+} available for downstream effects (Fig. 5). While the effects of acute treatment of osteoclast precursors by ATP on subsequent stimulation of osteoclastogenesis by RANKL have been previously described, to our knowledge this study is the first to report that short-term exposure to RANKL can change calcium response to a different mediator, such as ATP. (8) It can be hypothesized that long-lasting Ca^{2+} oscillations induced by RANKL interfere with the activity of plasma membrane or endoplasmic reticulum Ca^{2+} pumps, thus preventing effective calcium removal from the cytosol and resulting in a longer-duration response to ATP.

Further investigation is required to better understand the regulation of calcium oscillations induced by acute and long-term exposure to RANKL, as well as the implication of the differences in short term signaling for the physiological outcomes of osteoclast differentiation and function. Moreover, the potential role of RANKL-induced signaling on the calcium responses to other mediators, such as ATP, needs to be explored. Better understanding of osteoclast physiology will help in developing new diagnostic and therapeutic approaches in treating various bone diseases that are characterized by excessive osteoclastic bone resorption.

Acknowledgements

I would like to express my gratitude to Dr. Gulzhakhan Sadvakassova and Dr. Svetlana Komarova for the opportunity to work on this project, for their assistance and guidance, and to Antonio Rosario for help with frequency analysis.

References

1. Rodan G. Therapeutic Approaches to Bone Diseases. Science. 2000;289(5484):1508-1514.
2. Komarova S, Fong J. Breast Cancer Metastases to Bone: Role of the Microenvironment. In: Gunduz M, Gunduz E, ed. by. Breast Cancer - Focusing Tumor Microenvironment, Stem cells and Metastasis. 1st ed. InTech; 2011. p. 531-543.
3. Hwang S, Putney J. Calcium signaling in osteoclasts. Biochimica et Biophysica Acta (BBA) - Molecular Cell Research. 2011;1813(5):979-983.
4. Barreto-Chang O, Dolmetsch R. Calcium Imaging of Cortical Neurons using Fura-2 AM. Journal of Visualized Experiments. 2009;(23).
5. Yu H, Ferrier J. ATP Induces an Intracellular Calcium Pulse in Osteoclasts. Biochemical and Biophysical Research Communications. 1993;191(2):357-363.
6. Uhlen P. Spectral Analysis of Calcium Oscillations. Science Signaling. 2004;2004(258):pl15-pl15.
7. Takayanagi H, Kim S, Koga T, Nishina H, Isshiki M, Yoshida H et al. Induction and Activation of the Transcription Factor NFATc1 (NFAT2) Integrate RANKL Signaling in Terminal Differentiation of Osteoclasts. Developmental Cell. 2002;3(6):889-901.
8. Buckley K, Hipkind R, Gartland A, Bowler W, Gallagher J. Adenosine triphosphate stimulates human osteoclast activity via upregulation of osteoblast-expressed receptor activator of nuclear factor- κ B ligand. Bone. 2002;31(5):582-590.